Available online at www.sciencedirect.com
SCIENCE DIRECT
Journal of Catalysis 233 (2005) 288–296
JOURNAL OF CATALYSIS
www.elsevier.com/locate/jcat

Addition of hydrogen sulfide to methyl acrylate over solid basic catalysts

Emmanuelle Breysse [a], François Fajula [a], Annie Finiels [a], Georges Frémy [b], Didier Tichit [a], Claude Moreau [a,*]

[a] *Laboratoire de Matériaux Catalytiques et Catalyse en Chimie Organique, UMR 5618 CNRS-ENSCM-UM1, Ecole Nationale Supérieure de Chimie, 8, Rue de l'Ecole Normale, 34296 Montpellier cedex 5, France*
[b] *Groupement de Recherches de Lacq ATOFINA, BP 34, 64170 Lacq, France*

Received 1 February 2005; revised 21 April 2005; accepted 1 May 2005

Available online 6 June 2005

Abstract

H_2S was added to methyl acrylate in a batch reactor at 313 K, 450 rpm, 0.2 M (in decane) in methyl acrylate, 5.5 bar of hydrogen sulfide pressure in the presence of solid bases. The bases differed in their chemical composition, structural properties, and acid–base properties. The bases were cation-exchanged X-faujasites, magnesium oxide, alkaline- and alkaline-earth-doped magnesium oxides, and commercially available and synthesized mixed magnesium/aluminum oxides. All of these catalysts were shown to achieve, in terms of both activity and selectivity, the addition of H_2S to methyl acrylate as compared with the patent literature. Catalytic runs have also been conducted on a fixed-bed continuous-flow reactor with performances, in terms of selectivity, better than those observed in batch mode, particularly with a Cs-exchanged X zeolite, which featured a selectivity level similar to that of modified ion-exchange resins. As previously assumed from kinetics and IR studies on H_2S and methyl acrylate adsorption and co-adsorption, the prerequisite for the title reaction to occur is the dissociation of H_2S into HS^- and H^+ species over weak acid/strong basic Lewis pair sites. This assumption is confirmed in this work and is in agreement with the HSAB principle; H_2S is dissociated into a soft HS^- nucleophilic species associated with a soft M^{x+} acid, and the hard H^+ species is associated with the hard O^{2-} basic species.

Keywords: Aldolization; Michael addition; Base catalysis; Hydrotalcites; Cation-exchanged X-faujasites; Magnesium oxides; Alkaline- and alkaline-earth-doped magnesium oxides

1. Introduction

Methyl-3-mercaptopropionate (MMP) is of primary importance as a feedstock for the production of various industrial chemicals, pharmaceuticals, and agrochemicals, as indicated by a significant number of patents granted in the period from the 1970s to the 1990s that used homogeneous catalysts [1–7]. For practical and environmental reasons, most of the companies involved in this area have considered this reaction in the presence of solid bases, namely anion-exchanged resins, basic oxides, and hydroxides [8–11]. Satisfactory selectivities in MMP were generally claimed, between 82 and 97%, depending on the operating conditions and catalysts used; the highest selectivity has been obtained under high H_2S pressure, where H_2S is partially liquid and plays the role of solvent [9]. However, a high selectivity for MMP is generally achieved in the presence of a large excess of H_2S, whatever the catalysts used.

MMP is obtained through the nucleophilic Michael-type reaction addition of H_2S to methyl acrylate (MA) over basic catalysts (Scheme 1, Eq. (1)). Apart from MMP, dimethyl 3,3′-thiodipropionate (DMTDP) is the main secondary product, resulting from the addition of MMP to methyl acrylate (MA) (Scheme 1, Eq. (2)). Other side-reactions may also take place, namely the condensation of two molecules of MMP to give the corresponding disulfide and polymerization of methyl acrylate.

* Corresponding author. Fax: +33 (0)467 163 470.
E-mail address: claude.moreau@enscm.fr (C. Moreau).

0021-9517/$ – see front matter
doi:10.1016/j.jcat.2005.05.002

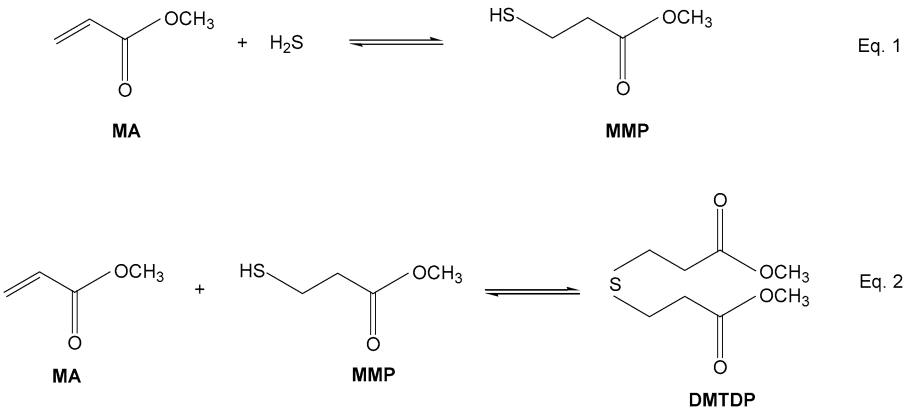

Scheme 1. Reaction scheme for the base-catalyzed addition of H_2S to methyl acrylate.

Resins exchanged with tertiary amines or quaternary ammonium ions were not found to be stable enough. However, an increase in both stability and efficiency was found with the use of guanidine-grafted resins [11]. MMP is produced in a continuous process without solvent, with a selectivity of 98% at 318 K and a H_2S/MA molar ratio of 6.

In a recent work we reported on a detailed study (kinetics, FT-IR adsorption, and coadsorption experiments) of the mechanism of the addition of H_2S to methyl acrylate in the presence of a commercial hydrotalcite (KW2200 from Kyowa) and magnesium oxide as catalysts. Under this chemical regime, it was shown that chemisorbed H_2S species like HS^-, which result from H_2S dissociative adsorption, were the active species and that strongly adsorbed MA was not involved in the reaction [12]. It was then anticipated that selective and active catalysts should contain weak Lewis acid/strong base pairs.

In order to corroborate the conclusion of our kinetic approach, the goal of the work reported in this paper was to perform the title reaction with a series of catalysts ensuring a large range of basicity regarding, on one hand, the Brønsted or Lewis nature of their sites, and on the other hand, the very different strength of the Lewis-type acid–base pairs. For this purpose alkaline-exchanged X zeolites, Mg(Al)O mixed oxides obtained from hydrotalcite precursor, meixnerite, and alkaline- or alkaline-earth-doped MgO were investigated. They indeed cover a wide range of basic strength, from weak for X zeolites [13] to moderate and strong for Mg(Al)O mixed oxides and very strong for doped MgO. Furthermore, meixnerite, in contrast to previous samples, exhibits Brønsted-type basic sites assigned to the OH^- compensating anions of this lamellar structure.

2. Experimental

2.1. Reactants

MA (99% purity) and dimethyl 3,3′-thiodipropionate (99% purity) were obtained from Aldrich, MMP (98% purity) from Fluka, decane (99+% purity, solvent) and dodecane (99+% purity, internal standard) from Interchim, and hydrogen sulfide (99.8% purity) from AGA.

2.2. Sample characterization

Chemical analyses of the as-prepared solids were performed at the Service Central d'Analyses du C.N.R.S. (Solaize, France) by ICP-MS.

X-ray diffraction patterns were obtained on a powder X-ray Philips PW1380 diffractometer with Cu-K_α radiation ($\lambda = 1.540$ Å, 40 kV and 50 mA).

Specific surface areas (BET method) and pore volumes were calculated from the isotherms of nitrogen adsorption/desorption recorded at 77 K with a Micromeritics ASAP 2010 M apparatus. Samples ($\approx$100 mg) were calcined at 723 K and outgassed at 523 K and 10^{-4} Pa.

The total basicity of the catalysts was measured by thermal adsorption and desorption of CO_2 with a Setaram TG-DSC-111 microcalorimeter. The samples were previously outgassed at 723 K, cooled to 373 K, and brought into contact with flowing CO_2 (25 ml min^{-1}). The thermal event in the microcalorimetric cell was recorded.

The total acidity of the catalysts was measured by adsorption of deuterated acetonitrile followed by IR spectroscopy with a Nicolet FTIR 320 spectrometer. The IR spectra were recorded at room temperature at a resolution of 2 cm^{-1} (100 scans). The samples were pressed into a disk wafer of 11 mg cm^{-2}. The activation was performed in oxygen flow (150 ml min^{-1} at 773 K for 8 h, then evacuated at the same temperature and a pressure of 1.33×10^{-4} Pa. After evacuation at 773 K, the sample was cooled to room temperature, and CD_3CN was admitted to the cell, at full coverage, then evacuated either at room temperature or at 333 K. IR spectra were then recorded.

2.3. Workup procedure

The procedure was typically as follows: 50 ml of decane containing MA (0.870 g, 0.01 mol) and dodecane (0.850 g, 0.005 mol) was poured into a 0.1-liter magnetically stirred

autoclave (Autoclave-Engineers). The freshly activated catalyst (≈ 100 mg) was kept under a nitrogen atmosphere until its fast transfer into the reaction medium, thus avoiding its exposure to air. The reactor was closed, purged with nitrogen, and cooled at 273 K. Then, H_2S gas was introduced under stirring (450 rpm) to the required pressure (5.5 bar), and the reactor was heated to 313 K. Zero time was taken to be when the temperature reached 313 K. Experimental conditions were close to those used in the French patent [11], that is, at a conversion of MA of 40%, and in such a manner that the reaction rates were not influenced by external and internal diffusional limitations.

The behavior of selected catalysts was also investigated with the use of a fixed-bed continuous-flow reactor in the absence of solvent under the following conditions: 4 g of catalyst (125–250 µm), 1.5 mol l^{-1} of MA, a MA/H_2S molar ratio of 6, 313 K [11].

2.4. Analyses

Samples were periodically withdrawn and analyzed by gas liquid chromatography (Hewlett–Packard 6890 gas chromatograph equipped with a flame ionization detector; HP5 capillary column (30 m × 0.32 mm, 0.25-µm film thickness, hydrogen as carrier gas), from 313 to 523 K, 30 K min^{-1}). Reaction products were identified by comparison with authentic samples. The initial reaction rates (mean value of three runs) were deduced from the experimental curves of concentrations versus time by determination of the slope at the origin. Reaction rates are normalized to the specific surface area in order to take into account the variation in the surface areas for all catalysts and the variation in pore volumes for zeolites.

3. Catalyst preparation and characterization

3.1. Cation-exchanged zeolites

KX, RbNaX, and CsNaX zeolites have been prepared by ion exchange at room temperature of the parent NaX zeolite from Aldrich (Si/Al = 1.33) with aqueous solutions of KCl, $RbNO_3$, and CH_3COONH_4 followed by CH_3COOCs for CsNaX. Their cationic content and textural properties are listed in Table 1. Specific surface areas and pore volumes obtained are in agreement with those reported in the literature [14] and decrease when Na^+ is replaced by K^+, Rb^+, or Cs^+, because of the increase in the cation radius.

By XRD analysis, it is verified that the structure of the starting material is not affected by the exchange procedure. These patterns are indeed characteristic of a well-crystallized NaX faujasite structure [15]. Nevertheless, the intensity of the peaks at around $2\theta = 6°$, 10°, 15°, 23° and 31° decreases when Na^+ is replaced by K^+, Rb^+, or Cs^+, respectively, because of a greater structural disorder induced by the position of the cations.

Table 1
Chemical composition and textural properties of cation-exchanged X-faujasites

Catalyst	% of cation exchange	Surface area[a] ($m^2\ g^{-1}$)	Pore volume ($cm^3\ g^{-1}$)	Cation radius (Å)
NaX	100 (Na)	666	0.314	Na = 0.97
KX	98.5 (K) 1.5 (Na)	581	0.275	K = 1.33
RbNaX	64 (Rb) 36 (Na)	473	0.224	Rb = 1.47
CsNaX	68 (Cs) 32 (Na)	371	0.168	Cs = 1.67

[a] Activation at 773 K under air flow for 6 h, then outgassed at 523 K.

Table 2
Chemical composition and specific surface area of hydrotalcites HT(0.25), HT(0.31) and HT(0.34)

Catalyst	Chemical composition	Surface area[a] ($m^2\ g^{-1}$)
HT(0.25)	$Mg_{0.75}Al_{0.25}(OH)_2(CO_3^{2-})_{0.103}(NO_3^-)_{0.08}\cdot mH_2O$	208
HT(0.31)	$Mg_{0.69}Al_{0.31}(OH)_2(CO_3^{2-})_{0.14}(NO_3^-)_{0.04}\cdot mH_2O$	318
HT(0.34)	$Mg_{0.66}Al_{0.34}(OH)_2(CO_3^{2-})_{0.153}(NO_3^-)_{0.03}\cdot mH_2O$	180

[a] Activation at 873 K under N_2 flow for 6 h, then outgassed at 523 K.

3.2. Hydrotalcites

Three hydrotalcite samples with an aluminum molar fraction of Al/(Mg + Al) = 0.25, 0.31 and 0.34 have been prepared with a coprecipitation procedure at a constant pH of 10 [16]. Their chemical composition (Table 2) and XRD patterns are characteristic of pure and highly crystallized lamellar phases. A thermal treatment of these structures induces, as already described [17], dehydration, dehydroxylation, and decomposition of anions, leading to a Mg(Al)O mixed oxide structure.

The influence of the temperature of calcination on both the structural and textural properties of HT(0.31) has been particularly followed. The characteristic XRD pattern of the lamellar structure changes above 473 K to that of the mixed oxide, becoming more crystalline when the temperature increases to 1073 K. In the same temperature range the specific surface area and pore volume pass through a maximum at around 823 K.

3.3. Meixnerite form of hydrotalcites

The meixnerite form of the hydrotalcite HT(0.31) (i.e., the lamellar structure with OH^- as compensating anions) was prepared by decomposition of the precursor at 723 K for 6 h under nitrogen flow to obtain the mixed-oxide form, followed by rehydration at room temperature under a flow of water vapor for 7 days to take advantage of the so-called memory effect. The XRD pattern of this sample shows that the lamellar structure has been restored with a slight loss of the crystalline character compared to the HT(0.31) precursor.

Table 3
Chemical composition and specific surface area of alkaline and alkaline-earth doped magnesium oxides

Dopant	Precursor salt	Wt% cation g^{-1} [a]	10^4 mol of cation g^{-1} [b]	Surface area [c] ($m^2\,g^{-1}$)
None	–	–	–	240
Li	hydroxide	0.48	10	103
Na	hydroxide	0.44	2.7	156
K	hydroxide	0.48	1.7	179
Rb	nitrate	0.46	0.78	166
Cs	hydroxide	0.47	0.5	202
Ca	hydroxide	1.23	4.4	222
Sr	nitrate	0.49	0.79	222
Ba	hydroxide	0.4	0.42	234

[a] Elemental analysis before thermal treatment.
[b] Calculated taking into account the weight loss due to activation at 823 K.
[c] Activation at 823 K under air flow for 6 h, then outgassed at 523 K.

3.4. Magnesium oxide and doped magnesium oxides

Alkaline and alkaline-earth oxides are generally prepared from their hydroxide or carbonate form. The nature and the strength of the basic sites depend on the temperature of calcination, as for the mixed oxides [18,19].

The starting magnesium oxide was obtained by calcination of magnesium hydroxide at 823 K for 6 h under air flow. As the specific surface area and the number of basic sites of doped materials were shown to pass through a maximum for a low metal content [20], doped magnesium oxides, containing around 0.5 wt% Li, Na, K, Rb, Cs, Ca, Sr, and Ba, were prepared by impregnation with aqueous solutions of their nitrate or hydroxide precursor, followed by drying at 353 K under vacuum for 8 h. The nature of the salts used for impregnation, cation amounts, and specific surface areas are listed in Table 3.

It is observed from this table that the specific surface areas of alkaline-doped magnesium oxides fall in the range from 100 to 200 $m^2\,g^{-1}$ and are therefore smaller than that of bulk magnesium oxide (240 $m^2\,g^{-1}$), whereas those of alkaline-earth doped magnesium oxides are nearly similar.

Because of the low content of dopant added, no fundamental change is observed in the XRD spectra of the different doped magnesium oxides with respect to the parent MgO sample.

4. Results

4.1. Catalytic results

The initial specific activities and selectivities in MMP obtained for the different samples in a batch reactor at a conversion of 40% MA are listed in Table 4.

Each series of samples shows at very different activity level. The activity is indeed one order of magnitude higher for alkaline- and alkaline-earth-doped MgO than for cation-exchanged X zeolites. The sequence of activity for the different types of catalysts is then the following: alkaline- and alkaline-earth-doped MgO > Mg(Al)O > cation-exchanged X zeolites > meixnerite.

Table 4
Experimental results summary: catalysts, calcination temperature, initial activity, methyl 3-mercaptopropionate selectivity, cation radii

Entry	Catalyst	T calcination (K)	Initial activity ($\times 10^8$ mol $s^{-1}\,m^{-2}$)	MMP selectivity at 40% MA conversion	Cation radius (Å)
1	NaX	773	1.0	77	0.97 (Na)
2	KX	773	2.6	79	1.33 (K)
3	$Rb_{64}Na_{36}X$	773	2.4	81	1.47 (Rb)
4	$Cs_{68}Na_{32}X$	773	4.0	83	1.67 (Cs)
5	HT(0.31)	473	11.9 **(1.0)**[a]	82	
6	HT(0.31)	573	11.9	75	
7	HT(0.31)	723	13.4	68	
8	HT(0.31)	823	14.4 **(4.6)**[a]	64	
9	HT(0.31)	1073	14.0	62	
10	MgO	873	13.6	80	
11	HT(0.25)	873	13.0	68	
12	HT(0.31)	873	18.0	64	
13	HT(0.34)	873	10.0	60	
14	γ-Al_2O_3	873	9.6	61	
15	Meixnerite		– **(0.6)**[a]	68	
16	MgO	823	15	76	
17	MgO–Li	823	23	71	0.68 (Li)
18	MgO–Na	823	39	78	0.97 (Na)
19	MgO–K	823	26	83	1.33 (K)
20	MgO–Rb	823	20	77	1.47 (Rb)
21	MgO–Cs	823	26	80	1.67 (Cs)
22	MgO–Ca	823	30	75	0.99 (Ca)
23	MgO–Sr	823	27	80	1.12 (Sr)
24	MgO–Ba	823	14	77	1.33 (Ba)

[a] $\times 10^5$ mol $s^{-1}\,g^{-1}$ (As the surface area of meixnerite cannot be measured, initial reaction rates are compared on a catalyst weight basis).

Several significant features in Table 4 are worth noting:

(i) For the cation-exchanged X zeolites, the initial specific activity increases with the ionic radius of the alkaline cation (entries 1–4). The influence of the ionic radius is less straightforward in the case of MgO-doped catalysts: a slight decrease is observed for the alkaline-doped MgO (entries 17–21), whereas it decreases for the alkaline-earth-doped MgO (entries 22–24).

(ii) The initial specific activity depends on the calcination temperature and the Al molar fraction for the Mg(Al)O mixed oxides. The initial activity goes through a maximum after calcination at around 823 K (entry 8). Furthermore, when the different mixed oxides are compared, their initial activities are close to those of Al_2O_3 and MgO at high and low Al contents (entries 11 and 13). The initial activity of the mixed oxide is intermediate between those of the parent MgO and γ-Al_2O_3 oxides, and a remarkable maximum is observed for a molar Al fraction of about 0.3 (entry 12). Such a maximum has already been reported [21,22], for which the

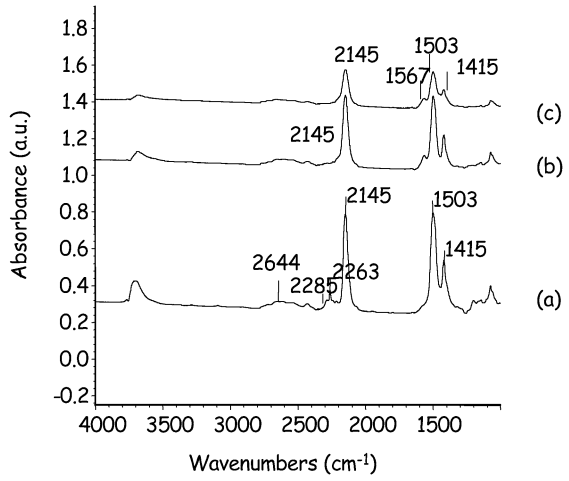

Fig. 1. Adsorption CD_3CN over MgO: (a) introduction of CD_3CN (6 Torr) at 293 K, (b) evacuation at 293 K, (c) evacuation at 333 K.

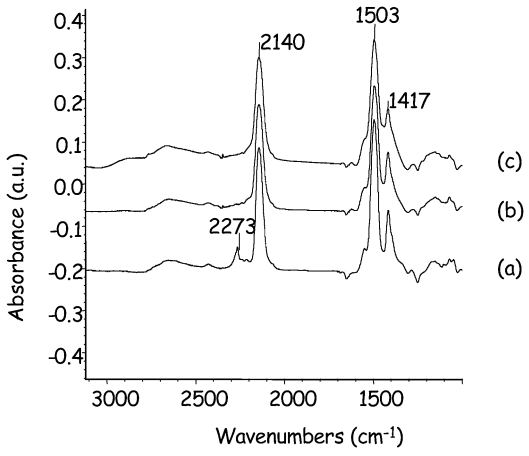

Fig. 2. Adsorption CD_3CN over MgO–Na: (a) introduction of CD_3CN (6 Torr) at 293 K, (b) evacuation at 293 K, (c) evacuation at 333 K.

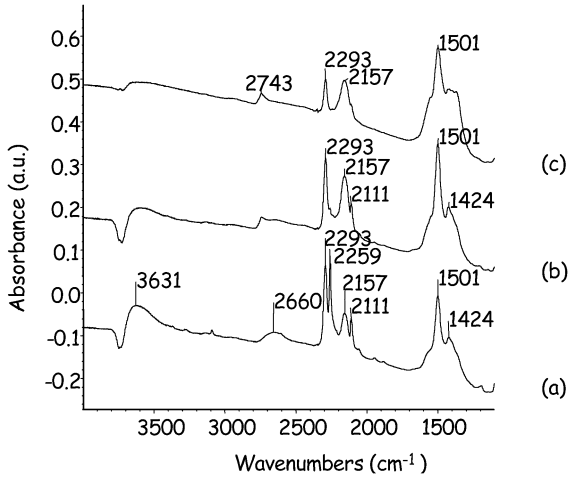

Fig. 3. Adsorption of CD_3CN over the mixed oxide $Mg_{0.69}(Al_{0.31})O$: (a) introduction of CD_3CN (6 Torr) at 293 K, (b) evacuation at 293 K, (c) evacuation at 333 K.

composition is supposed to correspond to that of the true mixed oxide.

(iii) The initial specific activity obtained with the meixnerite is very low. Meixnerite is by far the least active catalyst (entry 15) compared with the mixed oxide HT(0.31) calcined at low (entry 5) or high (entry 8) temperature.

The results of Table 4 show that the Brønsted-type sites present in the meixnerite sample are poorly active in the reaction [23]. This is also confirmed by the weak activity of the mixed oxide calcined below 723 K (entries 5 and 6) that are still partially hydroxylated.

Less straightforward correlations could be established between selectivities for MMP and the nature of the cations, and the activation temperature and the nature of sites. On one hand, it is worth noting that high selectivities are obtained with the most active cation-doped MgO samples. On the other hand, despite its low activity, meixnerite also exhibits low selectivity.

4.2. *Characterization of the acid–base properties*

As emphasized in the Introduction, the solids used for this study were chosen because of their different acid–base properties, and the preceding results actually indicate different behaviors in the catalytic reaction. In order to get more insight into the relationship between catalytic behavior and acid–base properties, representative samples, such as MgO, Na-doped MgO, $Mg_{0.69}(Al_{0.31})O$, and Al_2O_3, have been characterized by acetonitrile adsorption followed by IR spectroscopy.

Acetonitrile is an amphoteric probe well suited to elucidating the nature and eventually evaluating the strength of surface Lewis or Brønsted basic and acidic sites [24].

IR spectra obtained after the introduction of CD_3CN over the catalysts calcined at 773 K are reported in Figs. 1–4, with particular emphasis on the spectral range of 2400–2000 cm^{-1}, characteristic of $\nu(C{\equiv}N)$ vibration modes, because all of the surface species feature characteristic signals in this region.

MgO and Na-doped MgO show very similar behaviors. The $\nu(C{\equiv}N)$ modes in the 2230–2050 cm^{-1} spectral region are assigned to the CD_2CN^- and/or to polymeric anions formed on strongly basic O^{2-} sites and adsorbed thereafter to adjacent cationic sites [24–26].

The weak bands at 2285 and 2273 cm^{-1} on MgO (Fig. 1) and Na-doped MgO (Fig. 2), respectively, which totally vanish after desorption at 333 K, are due to CD_3CN N-bonded to Mg^{2+} Lewis acid sites [26,27].

It is worth noting that after evacuation at 333 K the intensities of the bands at 2140–2145 cm^{-1} remain higher on Na-doped MgO than on MgO, revealing a stronger basic strength of the former sample.

IR bands characteristic of the adsorption of CD_3CN on both basic and acid sites are also found on $Mg_{0.69}(Al_{0.31})O$ (Fig. 3). However, the important feature is that they exhibit an intensity ratio very different from that of the pre-

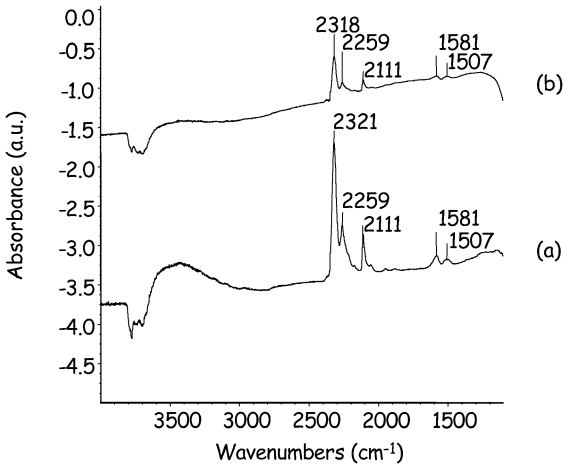

Fig. 4. Adsorption of CD_3CN over γ-Al_2O_3: (a) introduction of CD_3CN (6 Torr) at 293 K, (b) evacuation at 293 K.

vious samples. Indeed, CD_3CN adsorbed on the Lewis acid sites gives rise to a band with a stronger intensity shifted to higher frequency (i.e., at 2293 cm^{-1}). In contrast to MgO or Na-doped MgO, this band is maintained after evacuation at 333 K with an intensity rather similar to that of the basic species, giving a broad peak with a maximum at 2157 cm^{-1}. This typically shows that Mg(Al)O mixed oxides have an acid–base character that is attributed, on one hand, to the presence of Al^{3+} cations acting as stronger acid sites than Mg^{2+}, and, on the other hand, to O^{2-} basic sites. The intense band at 2259 cm^{-1} before evacuation was associated with both physisorbed and H-bonded acetonitrile [26].

Because of the well-known acidic character of Al_2O_3, the IR spectrum (Fig. 4) after adsorption at 273 K shows an intense band at 2321 cm^{-1} for CD_3CN N-bonded to Al^{3+} cations. Physisorbed and H-bonded species give rise to a band at 2259 cm^{-1} that is maintained after evacuation at 293 K. Furthermore, a broad band appears in the ν(OH) vibration range of 3000–3600 cm^{-1}, which confirms the presence of acetonitrile H-bonded to the surface. These features can be related to the presence of higher amounts of surface hydroxyls of higher acidity on alumina able to give H-bonded acetonitrile species. The characteristic bands of the anionic species present for the previous samples are not detected here.

The IR spectra previously described upon adsorption of the amphoteric CD_3CN probe were evidence of the evolution of acido-basicities from strong basic/weak acidic sites for Na-doped MgO and MgO to medium/strong acid and basic sites for Mg(Al)O mixed oxides and mainly acidic sites for γ-Al_2O_3. Moreover, it is known that the blue shift of the ν(C≡N) band of acetonitrile, which depends on the electron-withdrawing power of the cationic site, can be taken as a measure of the Lewis acid strength [28,29]. This order of strength for the previous catalysts is the following: γ-Al_2O_3 > $Mg_{0.69}(Al_{0.31})O$ > MgO > Na–MgO (Table 5). A rank of the catalysts regarding the basic strength is less straightforward because of the adsorption of acetonitrile on

Table 5
$CD_3CN\cdots M^{x+}$ frequencies and corresponding $\Delta\nu$(C≡N) shifts

Catalyst	Frequency of $CD_3CN\cdots M^{x+}$ species	$\Delta\nu$(C≡N)
None	2259 cm^{-1}	0 cm^{-1}
MgO	2285 cm^{-1}	25 cm^{-1}
Na-doped MgO	2273 cm^{-1}	14 cm^{-1}
HT(0.31)	2293 cm^{-1}	34 cm^{-1}
γ-Al_2O_3	2318 cm^{-1}	59 cm^{-1}

Table 6
Heats of CO_2 adsorption at 373 K

Catalyst	ΔH CO_2 (kJ mol^{-1})
Na-doped MgO	−78.2
MgO	−69.6
HT(0.31)	−60.3
γ-Al_2O_3	−52.8

Table 7
$CD_3CN\cdots M^{x+}$ frequencies, corresponding $\Delta\nu$(C≡N) shifts and heats of CO_2 adsorption at 373 K

Catalyst	ν(CN) (cm^{-1})	ΔH CO_2 (kJ mol^{-1})
$Cs_{68}Na_{32}X$		−49
$Mg_{0.69}(Al_{0.31})O$	2293 ($\Delta\nu = 34$)	−60
MgO	2285 ($\Delta\nu = 25$)	−70
MgO–Li		−77
MgO–Na	2273 ($\Delta\nu = 14$)	−78
MgO–K		−86
MgO–Rb		−88
MgO–Cs		−90
MgO–Ca		−68
MgO–Sr		−78
MgO–Ba		−85
γ-Al_2O_3	2318 ($\Delta\nu = 59$)	−53

acid–base pairs giving CH_2CN^- species and on O^{2-} and OH^- sites giving acetamide species. However, the evolution of intensity of the bands could not be disregarded and shows a net evolution of basic strength. Therefore a study of the basicity has also been performed by microcalorimetry with the use of adsorption of CO_2, whose heat of adsorption allows an evaluation of the basic strength. The results reported in Table 6 show that for the previous series of samples the basic strength is in the following order: Na–MgO > MgO > $Mg_{0.69}(Al_{0.31})O$ > γ-Al_2O_3.

This sequence is the reverse of the ranking established for the acid strength and is in agreement with the results already reported for IR spectroscopy of adsorbed acetonitrile. This confirmed that for these solids with coupled acid–base sites the individual strength of sites necessarily evolved in the opposite direction.

Interestingly, the heat of adsorption of CO_2 is also given for $Cs_{68}Na_{32}X$ and for the series of alkaline- and alkaline-earth-exchanged MgO samples in Table 7. Heats of adsorption listed in Tables 6 and 7 were obtained on samples previously treated at 723 K. TG analyses of these samples do not show any weight loss at temperatures higher than 723 K.

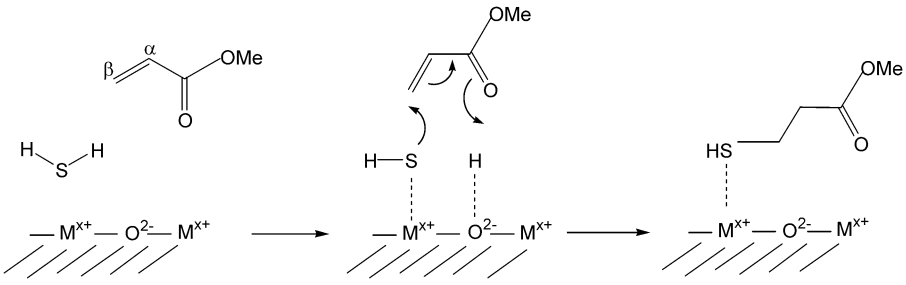

Scheme 2. Proposed reaction mechanism for the base-catalyzed addition of H_2S to methyl acrylate.

Therefore, we may assume that CO_2 is totally desorbed at this temperature and that stronger basic sites are not present. According to the literature [30], it has also been shown that the CO_2 desorption at temperatures above 773 K was negligible for Cs-exchanged faujasites. $Cs_{68}Na_{32}X$ exhibits a weak basic strength, in the same range as Al_2O_3, because of its high loading in Na^+. The basic strength increases with the cation size in the alkaline- and alkaline-earth-exchanged MgO samples. Similar behavior has already been reported [31–33] and was accounted for by the increasing electron-donating ability of the different alkaline and alkaline-earth oxides formed on the MgO support, which increases the average negative charge on the basic O^{2-} sites.

5. Discussion

We had previously determined from kinetics and further IR study on H_2S and MA adsorption and coadsorption that the prerequisite for this reaction was the dissociation of H_2S into HS^- and H^+ species over Lewis acid/base pair sites [12]. The HS^- species formed by the dissociation of H_2S on O^{2-} sites and adsorbed on the adjacent Lewis acid site is able to attack the terminal carbon atom of a MA species present in the surrounding liquid phase. This leads to a MMP molecule adsorbed on a Lewis acid site through the S atom, as we proposed in the mechanism given in Scheme 2.

Following this mechanism, the H abstraction on H_2S leading to HS^- species must be easier as the basic strength of the O^{2-} sites increases. Therefore one could expect an increase in the initial reaction rate with the basic strength of the catalysts evaluated by the heat of adsorption of CO_2. This is actually the case, as reported on Fig. 5 for the series of $Cs_{68}Na_{32}X$, Al_2O_3, $Mg_{0.69}(Al_{0.31})O$, MgO, and Na–MgO samples.

Regarding the cation-exchanged X zeolites, it has been established for a long time that the basic strength depends on the nature of the cations and increases in the order Li < Na < K < Rb < Cs (Table 8). In this table are also listed the values of the intermediate electronegativity, S_{int}, and of the partial oxygen charge, δ, which were calculated according to the principle of Sanderson [34]. Indeed, from microcalorimetric measurements based on the adsorption of acidic and basic probe molecules, the intermediate electronegativity, S_{int}, of the zeolite structure was shown by Auroux et al. [14] to be

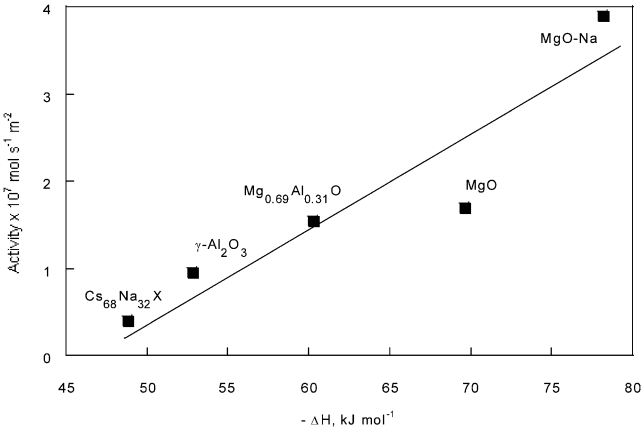

Fig. 5. Initial specific activities ($\times 10^7$ mol s^{-1} m^{-2}) of MgO and Na-doped MgO, both calcined at 823 K, hydrotalcite HT(0.31) and γ-alumina, both calcined at 873 K, and CsNaX zeolite calcined at 773 K, as a function of CO_2 adsorption heats (kJ mol^{-1}) measured at 373 K.

Table 8
Initial specific activity, MMP selectivity at 40% MA conversion, electronegativity (S_{int}), partial negative charge on oxygen atom (δ) and cation radius

Catalyst	Initial activity ($\times 10^8$ mol s^{-1} m^{-2})	MMP selectivity	Electronegativity (S_{int})	Oxygen charge (δ)	Cation radius (Å)
NaX	1.0	77%	2.404	−0.314	0.97 (Na)
KX	2.6	79%	2.335	−0.331	1.33 (K)
$Rb_{64}Na_{36}X$	2.4	81%	2.294	−0.342	1.47 (Rb)
$Cs_{68}Na_{32}X$	4.0	83%	2.220	−0.360	1.67 (Cs)

an indication of the Lewis acid strength of the cation, and the calculated oxygen charge, δ, to be an indication of the Lewis basic strength of the zeolites. It was also shown that the activity and selectivity of the reaction studied were both affected by the acid–base properties of the catalysts.

The increase in the catalytic activity from NaX to CsX is well correlated with the increase in the basic character of the cation-exchanged zeolites (Fig. 6), and the selectivity for MMP tends to decrease from CsX to NaX (Fig. 7). The existence of acid–base pairs is then important to considered with regard to both activity and selectivity.

A correlation of the same kind between the initial reaction rate and the nature of the cations was obviously expected regarding the MgO-doped samples. However, this is not strictly the case upon examination of the results reported in Table 4. This can be related to the different cation loading

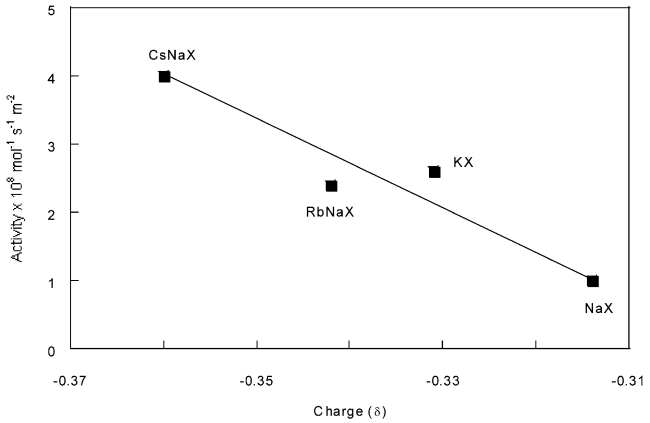

Fig. 6. Initial specific activity ($\times 10^8$ mol s^{-1} m^{-2}) against calculated partial oxygen charge for cation-exchanged X-faujasites.

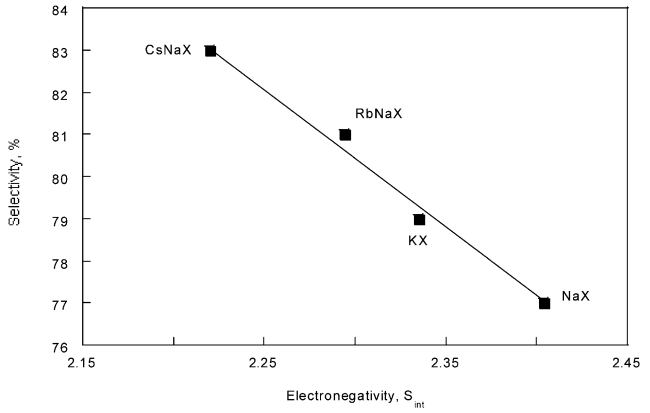

Fig. 7. MMP selectivity at 40% MA conversion against calculated intermediate electronegativity for cation-exchanged X-faujasites.

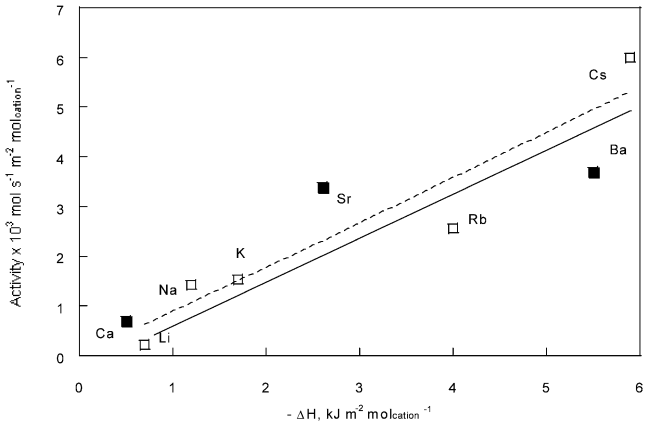

Fig. 8. Initial specific activity ($\times 10^3$ mol s^{-1} m^{-2} mol_{cat}^{-1}) versus heat of CO_2 adsorption (kJ m^{-2} mol_{cat}^{-1}) for alkaline (■) and alkaline-earth (□) doped MgO.

of the samples, which is a main factor influencing the surface basicity [31–33]. Indeed, one can note that the expected correlation with cation size is found when one considers the initial reaction rate per mole of cation (Fig. 8).

According to our proposed reaction scheme, it appears that the adsorbed MMP must be more rapidly desorbed when

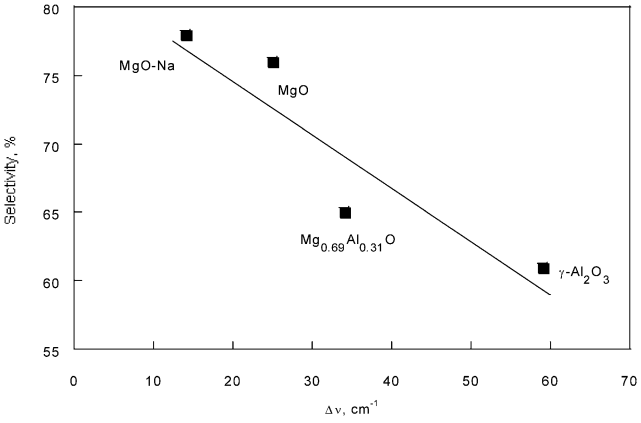

Fig. 9. MMP selectivity at 40% of MA conversion as a function of the difference $\Delta\nu$(C≡N) in the wavelength of Lewis acid coordinated CD_3CN and that of physisorbed CD_3CN.

the acid strength weakens and consequently induces an increase in selectivity. This tendency is confirmed when one examines the evolution of selectivities at 40% MA conversion for the Na-doped MgO, MgO, $Mg_{0.69}Al_{0.31}O$, and $Cs_{68}Na_{32}X$ samples as a function of the acid strength evaluated from the ν(C≡N) shift of adsorbed acetonitrile (Fig. 9). The highest selectivities in MMP at 40% MA conversion are obtained for MgO and doped MgO (Table 4, entries 10 and 16–24). Selectivities of only from 60 to 68% are obtained for the three mixed oxides, and a selectivity of 61% is obtained for γ-alumina (Table 4, entries 11–14).

6. Micropilot test

As summarized in Table 4 for the different series of catalysts studied, the highest selectivities in MMP were obtained over the cesium-exchanged zeolite and magnesium oxides, doped or not. H_2S was then added to MA with the use of a fixed-bed, continuous-flow reactor over those catalysts and over the basic ion-exchange Amberlyst A21 resin for comparison.

Under the operating conditions described in patent [11] (i.e., without solvent and with a larger amount of catalyst), it was confirmed that sodium-doped MgO was more active than the Cs-exchanged X zeolite and more active than the reference ion-exchange resin (Fig. 10).

However, from the comparison of the results obtained in another series of experiments in a batch reactor and those obtained in a continuous reactor, a higher selectivity in MMP is obtained over the Cs-exchanged X zeolite and the reference ion-exchange resin than over the sodium-doped MgO (Table 9).

It is then possible to anticipate that the new catalytic systems developed in this work with a batch reactor in the presence of a solvent should also demonstrate both high activity and high selectivity in MMP under continuous operation without solvent.

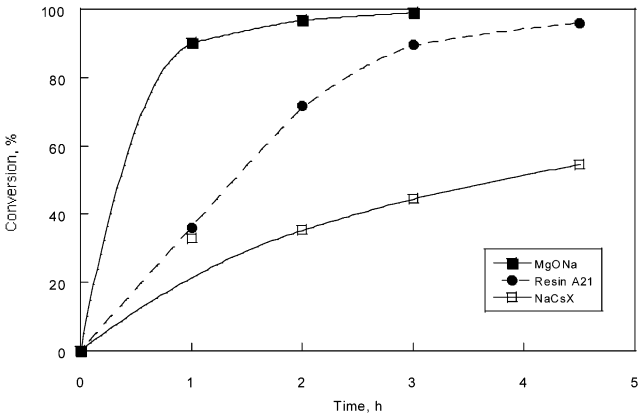

Fig. 10. Methyl acrylate conversion vs time for Na-doped MgO, ion-exchange A21 resin and Cs-exchanged X-faujasite (catalyst: 4 g, [MA]: 1.5 mol l^{-1}, [MA]/[H_2S] = 6, 313 K).

Table 9
Methyl 3-mercaptopropionate selectivity for batch and fixed bed continuous flow reactors

Catalyst	MMP selectivity at 50% MA conversion (batch)	MMP selectivity at 40% MA conversion (continuous flow)
$Cs_{68}Na_{32}X$	96%	84%
MgO–Na	72%	78%
Amberlyst A21	91%	79%

7. Conclusion

It has been shown in this work that basic solids, namely alkaline cation-exchanged X zeolites, magnesium–aluminium hydrotalcites, and alkaline- and alkaline-earth-doped magnesium oxides, a series of catalysts that were already known to differ in their chemical composition, structural properties, and acid–base properties, were capable of achieving the addition of H_2S to MA. Experiments have also been developed that use a continuous mode with a selectivity in MMP higher than that obtained with a batch mode.

We had previously determined from kinetics and further IR study of H_2S and MA adsorption and coadsorption that the prerequisite for this reaction was the dissociation of H_2S into HS^- and H^+ species over Lewis weak acid/strong basic sites [12]. This hypothesis was then confirmed in this work.

According to Scheme 2, and in agreement with the HSAB principle [35,36], H_2S would be dissociated into a soft HS^- nucleophilic species associated with a soft M^{x+} acid, and the hard H^+ species would be associated with the hard O^{2-} basic species.

Acknowledgments

The Groupement de Recherches de Lacq is gratefully acknowledged for financial support. E.B. thanks CNRS for a doctoral grant.

References

[1] S. Gladstone, S.R. Rao, C.J. Rosshirt, US Patent 4 052 440 (1977), to Witco Chemical Corporation.
[2] S. Gladstone, S.R. Rao, C.J. Rosshirt, US Patent 4 067 901 (1978), to Witco Chemical Corporation.
[3] R.P. Louthan, R.C. Doss, US Patent 4 113 707 (1978), to Phillips Petroleum.
[4] D.S. Sullivan, W.L. Bridges, US Patent 4 231 956 (1980), to Exxon Research Engineering.
[5] R.P. Louthan, US Patent 4 433 134 (1984), to Phillips Petroleum.
[6] H.Tatsumi, JP Patent 59 186 955 (1984), to Toyo Kasei Kogyo.
[7] D.R. Chisholm, G.A. Seubert Jr., EP patent 0 485 139 (1992), to Witco Chemical Corporation.
[8] A. Numata, R. Orita, DE Patent 3 614 065 (1986), to Toyo Kasei Kogyo.
[9] J.S. Roberts, US Patent 5 008 432 (1991), to Phillips Petroleum.
[10] Y. Hino, T. Wakao, T. Hayashi, JP Patent 6 298 724 (1994), to KK Nippon Shokubai.
[11] E. Arretz, FR Patent 2 756 282 (1988), to Elf-Aquitaine.
[12] E. Breysse, F. Fajula, A. Finiels, G. Frémy, J. Lamotte, F. Maugé, J.C. Lavalley, C. Moreau, J. Mol. Catal. A 198 (2003) 185.
[13] H. Hattori, Appl. Catal. A 222 (2001) 247.
[14] A. Auroux, P. Artizzu, I. Ferino, R. Monaci, E. Rombi, V. Solinas, Micropor. Mater. 11 (1997) 117.
[15] D.H. Olson, J. Phys. Chem. 74 (1970) 2758.
[16] K. Yamagushi, K. Ebitani, T. Yoshida, H. Yoshida, K. Kaneda, J. Am. Chem. Soc. 121 (1999) 4526.
[17] F. Cavani, F. Trifiro, A. Vaccari, Catal. Today 2 (1991) 11.
[18] K. Tanabe, H. Misono, Y. Ono, H. Hattori, Stud. Surf. Sci. Catal. 51 (1989) 27.
[19] S. Coluccia, A.J. Tench, Stud. Surf. Sci. Catal. 7B (1981) 1154.
[20] F.Q. Ma, D.S. Lu, Z.Y. Guo, J. Catal. 134 (1992) 644.
[21] M.J. Climent, A. Corma, S. Iborra, J. Primo, J. Catal. 151 (1995) 60.
[22] P.S. Kumbhar, J. Sanchez-Valente, J. Lopez, F. Figueras, Chem. Commun. (1998) 535.
[23] F. Prinetto, G. Ghiotti, R. Durand, D. Tichit, J. Phys. Chem. B 104 (2000) 11117.
[24] J.C. Lavalley, Catal. Today 27 (1996) 377.
[25] C. Binet, A. Jadi, J.C. Lavalley, J. Chim. Phys. 89 (1992) 31.
[26] F. Prinetto, M. Manzoli, G. Ghiotti, M.J. Martinez Ortiz, D. Tichit, B. Coq, J. Catal. 222 (2004) 238.
[27] H. Knözinger, H. Krietenbrik, J. Chem. Soc., Faraday Trans. I 71 (1975) 2421.
[28] J. Yarwood, Spectroscopy and Structure of Molecular Complexes, Plenum, London, 1973, p. 141.
[29] K.F. Purcell, R.S. Drago, J. Am. Chem. Soc. 88 (1966) 919.
[30] M. Laspéras, H. Cambon, D. Brunel, I. Rodriguez, P. Geneste, Micropor. Mater. 7 (1996) 61.
[31] J.I. Di Cosimo, V.K. Diez, C.R. Apesteguia, Appl. Catal. A 137 (1996) 149.
[32] J.I. Di Cosimo, V.K. Diez, M. Xu, E. Iglesia, C.R. Apesteguia, J. Catal. 178 (1998) 499.
[33] J.I. Di Cosimo, V.K. Diez, C.R. Apesteguia, Appl. Clay Sci. 13 (1998) 433.
[34] R.T. Sanderson, Chemical Bonds and Bond Energy, second ed., Academic Press, New York, 1976, p. 126.
[35] R.G. Pearson, in: R.G. Pearson (Ed.), Hard Soft Acids and Bases, Dowden, Hutchinson and Ross, Inc., Stroudbury, PA, 1973, p. 67.
[36] R.G. Pearson, H. Sobel, J. Songstad, in: R.G. Pearson (Ed.), Hard Soft Acids and Bases, Dowden, Hutchinson and Ross, Inc., Stroudbury, PA, 1973, p. 391.